

GEOMETRY OF FITNESS LANDSCAPES: PEAKS, SHAPES AND UNIVERSAL POSITIVE EPISTASIS

KRISTINA CRONA¹, JOACHIM KRUG², AND MALVIKA SRIVASTAVA³

ABSTRACT. Darwinian evolution is driven by random mutations, genetic recombination (gene shuffling) and selection that favors genotypes with high fitness. For systems where each genotype can be represented as a bitstring of length L , an overview of possible evolutionary trajectories is provided by the L -cube graph with nodes labeled by genotypes and edges directed toward the genotype with higher fitness. Peaks (sinks in the graphs) are important since a population can get stranded at a suboptimal peak. The fitness landscape is defined by the fitness values of all genotypes in the system. Some notion of curvature is necessary for a more complete analysis of the landscapes, including the effect of recombination. The shape approach uses triangulations (shapes) induced by fitness landscapes. The main topic for this work is the interplay between peak patterns and shapes. Because of constraints on the shapes for $L = 3$ imposed by peaks there are in total 25 possible combinations of peak patterns and shapes. Similar constraints exist for higher L . Specifically, we show that the constraints induced by the staircase triangulation can be formulated as a condition of *universal positive epistasis*, an order relation on the fitness effects of arbitrary sets of mutations that respects the inclusion relation between the corresponding genetic backgrounds. We apply the concept to a large protein fitness landscapes for an immunoglobulin-binding protein expressed in Streptococcal bacteria.

1. INTRODUCTION

This work on acyclic cube graphs and triangulations of cubes is motivated by applications to biology. Darwinian evolution can many times be analyzed by considering biallelic systems. For a biallelic L -locus system, a genotype g can be represented as a bit string of length L . The evolutionary potential for a genotype g is measured by its fitness. The fitness landscape $w : \{0, 1\}^L \mapsto \mathbb{R}_{\geq 0}$ is determined by the fitness values for all 2^L genotypes [9]. Recent approaches to fitness landscapes rely on analyzing L -cube graphs and triangulations that are induced by the landscapes [2].

One can give a complete (informal) description for $L = 2$. The four genotypes are denoted 00, 10, 01, 11. The induced graph on the square is determined by the condition that each arrow points toward the genotype of higher fitness (Figure 1). A Darwinian process starting from the genotype 00 corresponds to a path that respects the arrows. The graph 1C has two peaks (or sinks), which means that an evolving population can get stranded at a suboptimal peak.

The quantity $\epsilon = w_{11} + w_{00} - w_{10} - w_{01}$ measures the deviation of the fitness landscape from additivity known as epistasis [11, 20, 26]. If $\epsilon > 0$ the triangulation induced by the fitness landscape divides the square into

two triangles $\{00, 10, 11\}$ and $\{00, 01, 11\}$. If $\epsilon < 0$, the triangles are instead $\{00, 10, 01\}$ and $\{10, 01, 11\}$. For an intuitive understanding, if two genotypes do not belong to the same triangle, they could increase their average fitness by swapping positions $11 + 00 \mapsto 10 + 01$.

In general, we assume that the fitness landscape is generic in the sense of [1], and that no two genotypes have equal fitness. The graph determined by the fitness landscape, or the fitness graph [5, 10], is the acyclic L -cube graph defined by the condition that each edge is directed toward the genotype of higher fitness.

Following [1], let Δ be the simplex $\{p \in [0, 1]^{2^L} : \sum p_g = 1\}$, where p can be interpreted as the frequencies of the genotypes in a population, and $p \cdot w$ measures the average fitness of the population. Let $\rho : \Delta \mapsto [0, 1]^L$ be the map defined as $(\rho(p))_i = \sum_{g_i=1} p_g$. Note that ρ maps gene frequencies to allele frequencies, i.e, to the frequencies of 1's at a particular locus (or string position). Define

$$\tilde{w}(v) = \max_p \{p \cdot w : \rho(p) = v\} \text{ for all } v \in [0, 1]^L.$$

Then \tilde{w} is a piecewise linear function. The domains of linearity of \tilde{w} define a regular triangulation of $[0, 1]^L$ (because w is generic [8]). The triangulation is called the shape of the fitness landscape. Recent work on triangulations and fitness graphs includes [4, 6, 3, 7, 13, 12, 15, 19, 21].

Fitness graphs and shapes encode information of very different nature, and can be considered complementary [2]. However, there is also some overlap in the information. The peak pattern for a fitness landscape refers to the number of peaks and how they are positioned in the graph, up to cube symmetry. Some peak patterns impose constraints on the triangulations for $L = 2$ (Figure 1C) and $L = 3$ [30]. The main topic for this work is the interplay between peak patterns and triangulations. For the reader's convenience, a dictionary between terms used in biology and mathematics has been provided, see Table 3.

Main Results. For generic fitness landscapes $w : \{0, 1\}^L \mapsto \mathbb{R}_{\geq 0}$ we compare the induced peak patterns and triangulations. For $L = 3$ we show that there are exactly 25 possible combinations of peak patterns and triangulations (Theorem 1). The statistical distribution of peak patterns conditioned on the triangulation is obtained from simulations of random fitness landscapes. For higher L we show that some peak patterns are compatible with all triangulations, whereas other peak patterns are incompatible with almost all triangulations. A peak pattern and a triangulation are referred to as compatible if there exists a fitness landscape that induces both of them.

Of particular interest are fitness landscapes that are compatible with a staircase triangulation (Definition 1). We show that these landscape display a property that we call *universal positive epistasis*. The property holds if

$$(1) \quad w_{g \cup g'} + w_{g \cap g'} \geq w_g + w_{g'}$$

for all pairs of genotypes g and g' interpreted as sets of 1-alleles. It implies that the fitness effect of a given set of mutations on different genetic backgrounds inherits the partial order induced by the subset-superset relation

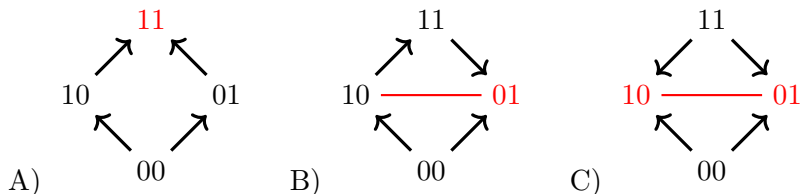


FIGURE 1. Fitness graphs for two loci under the assumption that 00 has minimal fitness. If the genotypes are positioned as in the figure, the three types can be characterized as graphs with all arrows up, one arrow down, and two arrows down. Peak genotypes are marked in red. Graphs B) and C) display sign epistasis [31], which means that at least one pair of arrows on parallel edges point in opposite directions. In graph C) sign epistasis is reciprocal [25]. Sign epistasis fixes the sign of the epistatic interaction ϵ and this constrains the triangulation. As a consequence, graphs B) and C) are compatible only with the triangulation indicated by the red lines.

between background genotypes. The conditions (1) characterize the staircase triangulation. Universal positive epistasis limits the maximal number of peaks in the fitness landscape, and explicit upper bounds are derived for $L = 4$ and $L = 5$. Gröbner bases for staircase triangulations (Theorem 2) were used for establishing that the bounds are sharp. The analysis of a large empirical data set of fitness interactions between protein substitutions selected for their positive epistatic effects [32] shows a significant overrepresentation of the staircase triangulation.

2. PEAK PATTERNS AND TRIANGULATIONS FOR $L = 3$

With notation as in the introduction, we consider fitness graphs and triangulations induced by the fitness landscape.

2.1. Classification results for $L = 3$.

Observation 1. *For $L = 3$ there are 5 peak patterns (Figures 2 and 3).*

- *Fitness graphs have 1-4 peaks.*
- *The peak pattern is unique if the number of peaks is 1, 3 or 4.*
- *There are two peak patterns if the number of peaks is 2. The distance between the peaks is either 2 or 3.*

A regular triangulation of the cube can be described as a subdivision of the cube into tetrahedra. It is well known that in the case of the 3-cube only 6 triangulations can arise, up to symmetries, see [8, Thm. 6.3.10]. The possible shapes are illustrated in Figure 4. The graphs below the cubes aid visual interpretations of the triangulations. The nodes of the graphs represent tetrahedra. Two vertices are joined by an edge if the corresponding tetrahedra have a triangle in common, and a shaded region indicates that the tetrahedra share a line segment. The graphs are defined as tight spans dual to the triangulations [17]. The corner tetrahedra (see the top row in

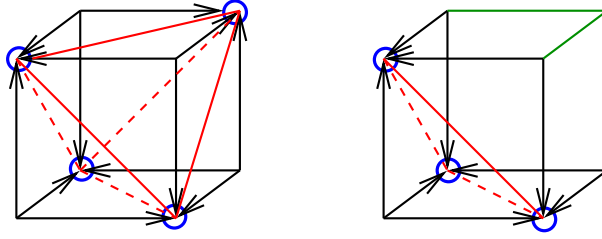


FIGURE 2. Three locus fitness graphs with 4 and 3 peaks. Face triangulations are indicated by full red lines for the exposed faces and dashed red lines for the hidden faces of the cube. Left panel: For the graph with 4 peaks, the peak pattern fully specifies the triangulation of the faces. The triangulation has to be of type 1 or 2 (these types have identical face triangulations, see Figure 4). Right panel: The presence of three peaks implies that a corner is isolated, which is inconsistent with type 6 triangulations.

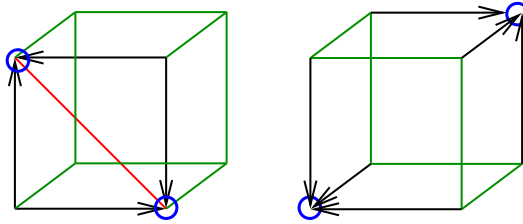


FIGURE 3. For graphs with two peaks, there are two possible peak patterns, depending on if the distance between the peaks is two or three. If the distance is two, the face triangulation is as indicated by the red line. Both cases are compatible with all six triangulations.

Figure 4) appear as nodes of degree 1 in the tight spans (i.e., nodes with only one outgoing edge).

Theorem 1. *The five peak patterns described in the previous observation, and the six triangulation types, as described in Figure 4, can be combined in 25 ways. Specifically*

- *Fitness graphs with 4 peaks are compatible with triangulations of type 1 and 2, but not with any other triangulations.*
- *Fitness graphs with 3 peaks are compatible with triangulations of type 1-5, but not with type 6.*
- *The remaining three peak patterns are compatible with all six triangulation types.*

Before giving the proof we introduce some formal notation for general L . In brief, a triangulation of the L -cube is a subdivision of the cube into $L+1$ -simplices (i.e., simplices that can be described as the convex hull of $L+1$ affinely independent points), such that any non-empty intersection between simplices are faces of both of them. For more background and definitions, see

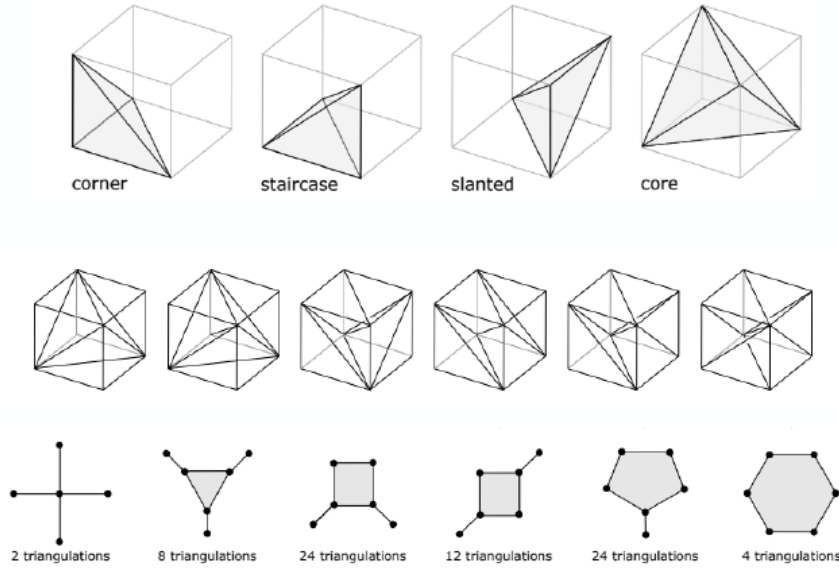


FIGURE 4. The six types of triangulations the 3-cube, together with the tight spans dual to the triangulations (modified from [24] with permission).

[8]. The triangulation induced by the fitness landscape w was defined in the introduction. In the terminology of [8], the triangulation is the projection of the upper envelope of the convex hull of the genotypes lifted by w . (For clarity, each genotype determines a point in \mathbb{R}^{L+1} by regarding w_g as a height coordinate. The triangulation is the projection of the upper faces of the polytope obtained as the convex hull of such points).

For $L = 3$, the triangulation divides each side of the cube along a diagonal. An inspection of such diagonals is useful for comparing triangulations and peak patterns. It is easy to verify that the diagonals marked red in Figures 2 and 3 are induced by the triangulation, since they connect peaks. For proving the theorem, it is helpful to introduce a new concept. We call a genotype g *isolated* if there is no genotype g' such that $\{g, g'\}$ belongs to the same simplex and $|g - g'| = 2$, i.e., no diagonal connects g to another genotype.

Remark 1. *If the triangulation slices off a genotype (see the bottom left vertex of the corner simplex in Figure 4) then the genotype is isolated. However, the converse is not true.*

The following observation follows by inspection of Figure 4.

Observation 2. *For the six triangulation types described in Figure 4,*

- *Type 1 triangulations have four isolated vertices.*
- *Type 2 triangulations have four isolated vertices.*
- *Type 6 triangulations have no isolated vertices.*

Peak pattern	Random landscapes	Isomorphism classes
1 peak	$\frac{3}{14} \approx 0.214$	$\frac{1}{2} = 0.5$
2 peaks at distance 2	$\frac{5}{14} \approx 0.357$	$\frac{5}{18} \approx 0.278$
2 peaks at distance 3	$\frac{1}{4} = 0.25$	$\frac{4}{27} \approx 0.148$
3 peaks	$\frac{1}{7} \approx 0.143$	$\frac{1}{18} \approx 0.055$
4 peaks (Haldane graph)	$\frac{1}{28} \approx 0.036$	$\frac{1}{54} \approx 0.0185$

TABLE 1. Distribution of peak patterns for random three-locus landscapes based on [28] and [4]. Decimal approximations of the exact rational probabilities are provided for convenience.

Proof of Theorem 1. If the fitness graph has 4 peaks, then the remaining four genotypes are isolated, which excludes the triangulations of types 3-6. If the fitness graph has three peaks, then the genotype adjacent to the three peaks is isolated, which excludes the type 6 triangulation. Out of the 30 combinations of peak patterns and triangulations, 5 are excluded as argued. The remaining 25 combinations of peak patterns and triangulations appear with nonzero probability in statistics for randomly generated fitness landscapes (see Section 2.2). \square

The constraints on triangulations imposed by the number of peak, as described in Theorem 1, agree with observations from simulations in [30] (Figure 5). Related results have been described in [29].

2.2. Peaks and shapes of random fitness landscapes. Generic random fitness landscapes are obtained by assigning independent, identically and continuously distributed random numbers to the genotypes [18]. Because peak patterns and fitness graphs are fully determined by the rank order of fitness values, the resulting statistics are independent of the underlying probability distribution. A simple rank order argument shows that the expected number of peaks of a random landscape over L loci is $\frac{2^L}{L+1}$, and the variance of the number of peaks is also known [22]. The full distribution of peak patterns for $L = 3$ was obtained in [28] and is reported in Table 1. Additionally the table shows the distribution of peak patterns over the 54 isomorphism classes of fitness graphs presented in [4].

Figure 5 shows the distribution of peak patterns conditioned on the triangulation type. In contrast to the statistics of fitness graphs presented in Table 1, these statistics depend on the probability distribution of fitness values [30]. The results in the figure were obtained using the uniform distribution on $[0, 1]$ (see Figure 6 for the distribution of triangulation types in this case).

The combinations of peak patterns and triangulation types excluded by Theorem 1 are absent in Figure 5, whereas all other combinations occur with positive probability. Furthermore, it can be seen that the overall ruggedness

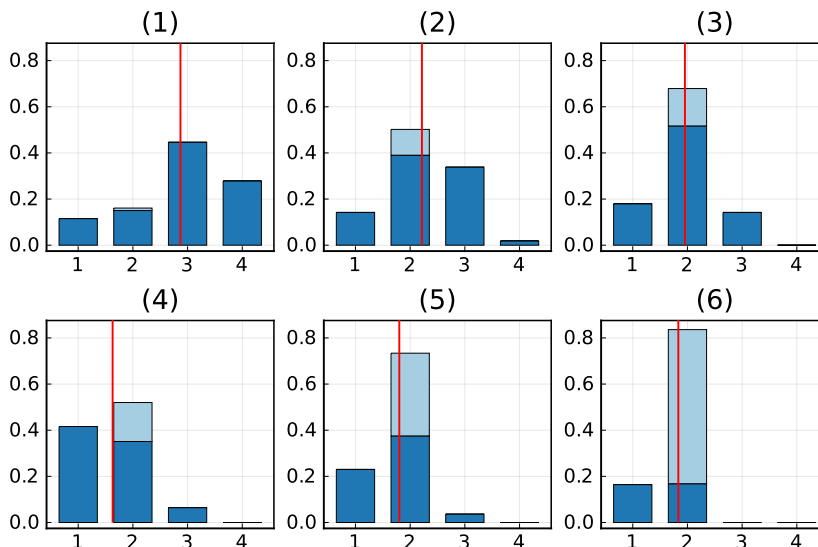


FIGURE 5. Distribution of the number of peaks for different triangulation types. The fitness values were taken to be uniformly distributed on $[0, 1]$. The vertical red lines indicate the mean of the distribution. For unconstrained random three-locus landscapes the mean number of peaks is 2. The light-blue portion of the bars at peak number 2 shows the fraction of landscapes where the two peaks are at distance 3.

of the landscapes (as measured, e.g., by the mean number of peaks) decreases systematically going from triangulation type 1 to type 6. A pronounced trend is observed for the patterns with two peaks: Whereas for triangulation type 1 the two peaks are almost exclusively at distance 2, for triangulation type 6 the pattern with two peaks at distance 3 dominates.

3. HIGHER DIMENSIONAL FITNESS LANDSCAPES

3.1. Extreme peak patterns and triangulations. A counting argument shows that the maximal number of peaks for a fitness graph is 2^{L-1} . This fact was first observed in [16], and we refer to these graphs as Haldane graphs. One can verify that each node in a Haldane graph is either a sink or a source.

Remark 2. *A fitness graphs has at most 2^{L-1} peaks. For graphs with the maximal number of peaks, each node is either a sink (peak) or a source. All neighbors of sinks are sources, and vice versa.*

Among graphs with only one peak, the all arrows up graph is defined as the graph where fitness increases by distance from the node with minimal fitness (if one draws the graphs as in Figure 1, all arrows point upward). One can verify that all arrows up graphs are compatible with all triangulations. The argument depends on the following construction: For a fitness landscape w and a constant $c \in \mathbb{N}$ let

$$w_g^{+c} = w_g + c \sum g_i.$$

For instance, $w_{00}^{+2} = w_{00}$, $w_{10}^{+2} = w_{10} + 2$, $w_{01}^{+2} = w_{01} + 2$, $w_{11}^{+2} = w_{11} + 4$. Consider an arbitrary triangulation of the L -cube induced by w . One verifies that the fitness landscapes w^{+c} and w induce the same triangulation. For sufficiently large c , the fitness graph corresponding to w^{+c} is an all arrows up graph.

Observation 3. *All triangulations are compatible with some single peaked fitness landscapes.*

Type 1 and type 6 triangulations can be considered opposite extremes for $L = 3$. The first triangulation slices off four genotypes, i.e., it has four corner simplices, and the latter does not slice off any genotypes. For general L , a corner simplex consists of a vertex g (the sliced off vertex) and its $L + 1$ neighbors [8]. Analogous to the $L = 3$ case, *corner-cut triangulations* are defined as triangulations that have 2^{L-1} corner simplices, i.e., the highest number of corner simplices for a given L [23]. Corner-cut triangulations are unique for $L = 3$ and $L = 4$ but not for general L [8].

The *staircase triangulation* is a direct generalization of the Type 6 triangulations. It is unique up to isomorphism. For notational convenience, we define the staircase triangulation such that each simplex contains the genotypes from a walk of length L from $00\dots 0$ to $11\dots 1$. All $L!$ walks are represented. For instance, for $L = 3$ the triangulation is

$$\begin{aligned} &\{000, 100, 110, 111\}, \{000, 100, 101, 111\}, \{000, 010, 110, 111\} \\ &\{000, 010, 011, 111\}, \{000, 001, 101, 111\}, \{000, 001, 011, 111\} \end{aligned}$$

Definition 1. *The staircase triangulation consists of $L!$ simplices, such that each simplex contains all genotypes from a walk of length L , starting at $00\dots 0$ (the zero string) and ending at $11\dots 1$.*

Also for general L , it is useful to consider the induced triangulations of two-dimensional faces. As for $L = 3$, such faces have no diagonals that connect isolated genotypes to other genotypes. Diagonals connect peaks on the two-dimensional faces for triangulations compatible with Haldane graphs. It follows that source genotypes are isolated. However, as already noted, they are not sliced off in general.

Remark 3. *The source genotypes are isolated for Haldane graphs.*

Consider the staircase triangulation for $L \geq 3$. For any genotype g , let g' be a genotype obtained by changing two loci (positions) from 1 to 0, or two loci from 0 to 1. Then g and g' belong to the same simplex, which implies that g is not isolated.

Remark 4. *If the fitness landscape induces the staircase triangulation, then there are no isolated genotypes.*

Observation 4. *Haldane graphs impose restrictions on triangulations to the extent that most triangulations are excluded.*

- (i) *Triangulations that are compatible with Haldane graphs have 2^{L-1} isolated genotypes.*
- (iii) *Haldane graphs are incompatible with staircase triangulations for $L \geq 3$.*

(iii) For any L , there exists a corner cut triangulation that is compatible with the Haldane graph.

Proof. (i) follows from Remark 3. (ii) follows from (i) and the previous remark. (iii) Consider a fitness landscape that induces a Haldane graph such that $w_g \approx 2$ for half of the genotypes and $w_g \approx 1$ for the remaining genotypes. One can verify that the fitness landscape induces a corner-cut triangulation provided the approximations are sufficiently close (by the generic assumption). \square

We have established that a Haldane graph is compatible with some corner-cut triangulation. A stronger claim would be that any corner-cut triangulation is compatible with the Haldane graph.

Open question: Are all corner-cut triangulations compatible with Haldane graphs?

3.2. Staircase triangulations and universal positive epistasis. It is sometimes convenient to use the set notation for genotypes [7]. If the bit-string representing the genotype has a 1 in position i , then the set contains the element $i \in \mathcal{L}$ of the locus set $\mathcal{L} = \{1, 2, \dots, L\}$. For $L = 2$, the translation is $00 = \emptyset$, $10 = \{1\}$, $\{0, 1\} = 2$, $\{11\} = \{1, 2\}$.

We consider the staircase triangulation as previously defined (Definition 1). For a pair of genotypes g, g' , let

$$X_{g,g'}(i) = \frac{1}{2}(g_i + g'_i).$$

In the terminology of [1], $X_{g,g'}(i)$ is the allele frequency vector of a population composed in equal part of g and g' , and such a population has fitness $\frac{1}{2}(w_g + w_{g'})$.

Assume that $g' \subset g$. Then g and g' belong to the same simplex in the staircase triangulation. Suppose that $\{h, h'\}$ is a pair of genotypes such that $X_{g,g'} = X_{h,h'}$. It is easy to verify that $h' \cup h = g$ and $h' \cap h = g'$. Unless the pair $\{h', h\}$ is identical to $\{g, g'\}$, one can exclude that $h' \subset h$ or $h \subset h'$, which shows that h and h' do not belong to the same simplex in the triangulation.

From these observations and properties of the fittest population described in [1] the following result is immediate.

Observation 5. Let g, g' be two genotypes where $g' \subset g$. Consider all pairs of genotypes $\{h, h'\}$ such that

$$X_{h,h'}(i) = X_{g,g'}(i),$$

The staircase triangulation implies that

$$w_g + w_{g'} \geq w_h + w_{h'},$$

with equality only if $\{h, h'\} = \{g, g'\}$.

To make contact with the usual definition of epistasis [11, 20, 26], let $b' \subset b \subset \mathcal{L}$, and let $s \subset \mathcal{L} \setminus b$. The previous observation applied to the genotypes $g = b \cup s$ and $g' = b'$ implies that

$$(2) \quad w_{b \cup s} - w_b \geq w_{b' \cup s} - w_{b'}.$$

In this formulation a set s of loci is added to two different backgrounds, b and b' , and the fitness effect of this substitution is larger in b than in b' if $b' \subset b$.

Definition 2 (*Universal positive epistasis*). *A fitness landscape displays universal positive epistasis if for any genotypes $b' \subset b \subset \mathcal{L}$ and set $s \subset \mathcal{L} \setminus b$, the inequality (2) holds.*

Equivalently, universal positive epistasis holds if the condition (1) is satisfied for any two genotypes g and g' or, if genotypes are represented as strings

$$w_{g \vee g'} + w_{g \wedge g'} \geq w_g + w_{g'}.$$

Informally, for a given allele frequency vector, one can construct the pair of genotypes with maximal fitness sum by distributing the 1's as unevenly as possible. For instance

$$w_{111} + w_{000} > w_{110} + w_{001}, w_{101} + w_{010}, w_{011} + w_{100}.$$

Conversely, a fitness landscape with universal positive epistasis induces the staircase triangulation, i.e, the condition is a characterization of the staircase triangulation (see Observation 9).

3.3. Peak patterns for the staircase triangulation. In this section single, double and triple mutants, and similarly, refer to the cardinality of the sets used in the set notation for genotypes. The zero string is represented by the empty set.

In the case of $L = 3$, fitness landscapes compatible with the staircase triangulation were found to be relatively smooth, and here we will show that this observation can be extended to general L . In particular, local conditions suffice to ensure that the landscape is single peaked.

Observation 6. *For fitness landscapes that induce the staircase triangulation the following statements hold:*

- (i) *If the zero string is a local fitness minimum it is also the global minimum and the fitness graph has all arrows up.*
- (ii) *If at most one of the L neighbors of the zero string has lower fitness the fitness landscape is single-peaked.*

Proof. (i) By assumption $w_i > w_\emptyset$ for all $i \in \mathcal{L}$. Since \emptyset is a subset of all genotypes, it follows from (2) that $w_{b \cup i} - w_b > 0$ for all background genotypes b . Thus all mutations are beneficial on all backgrounds and the fitness graph has all arrows up.

(ii) Suppose $w_j < w_\emptyset$ for some $j \in \mathcal{L}$ and $w_i > w_\emptyset$ for all $i \neq j$. Then $w_{b \cup i} - w_b > 0$ for all $i \neq j$, whereas $w_{b \cup j} - w_b$ may be positive or negative depending on the background b . Thus the fitness landscape displays at most one instance of sign epistasis (at locus j). Since the existence of multiple peaks requires a pair of loci with reciprocal sign epistasis [27], the landscape is single peaked. \square

The following properties of landscapes that induce the staircase triangulation are useful for counting peaks.

- (i) If a single mutant $\{i\}$ is a peak, then all other peaks contain $\{i\}$. In particular, two single mutants cannot both be peaks.

Proof. Suppose that $\{i\}$ and g are peaks, where $i \notin g$. Then $w_g > w_{g \cup \{i\}}$ and $w_i > w_\emptyset$. It follows that

$$w_{g \cup \{i\}} + w_\emptyset < w_i + w_g,$$

which contradicts (1). \square

- (ii) Two double mutants $\{i, j\}$ and $\{j, k\}$ that overlap cannot both be peaks.

Proof. Suppose that w_{ij} and w_{jk} are peaks, then $w_{ij} > w_j$ and $w_{jk} > w_{ijk}$. It follows that

$$w_{ijk} + w_j < w_{ij} + w_{jk}$$

which contradicts (1). \square

- (iii) A triple mutant $\{i, j, k\}$ and a double mutant $\{k, l\}$ that overlap cannot both be peaks.

Proof. Suppose that $\{i, j, k\}$ and $\{k, l\}$ are both peaks. Then $w_{ijkl} < w_{ijk}$ and $w_k < w_{kl}$. It follows that

$$w_{ijkl} + w_k < w_{ijk} + w_{kl}$$

which contradicts (1). \square

Observation 7. *If a fitness landscape induces the staircase triangulation, then there are at most four peaks if $L = 4$.*

Proof. The argument depends on the properties (i)-(iii). For $L = 4$, if a single mutant $\{i\}$ is a peak, then other peaks would have to be of the form $\{i, j, k\}$ or $\{i, j, k, l\}$ by (i). Consequently, there are most two peaks.

If a triple mutant is a peak, then there are at most two peaks by symmetry.

It only remains to consider the case when no single or triple mutants are peaks. If a double mutant $\{i, j\}$ is peak, then other peaks would have to be of the types \emptyset , $\{k, l\}$ or $\{i, j, k, l, m\}$ by (ii). Consequently, there are at most four peaks. \square

The following example shows that the bound for $L = 4$ is sharp.

Example 1. *Consider the fitness landscape where*

$$w_{0000} = 20, w_{1100} = 4, w_{0011} = 4, w_{1111} = 20,$$

$$w_{1010} = 1, w_{1001} = 1, w_{0110} = 1, w_{0101} = 1,$$

and all other genotypes have fitness 3. The four genotypes $w_{0000}, w_{1100}, w_{0011}$ and w_{1111} are peaks and the landscape induces the staircase triangulations. (See Section 4 for computational details).

Observation 8. *If a fitness landscape induces the staircase triangulation, then there are at most four peaks if $L = 5$.*

Proof. The argument is similar to the case $L = 4$. We subdivide the hypercube into layers of genotypes of the same cardinality k , where $0 \leq k \leq L$. Layers k and $L - k$ are equivalent by symmetry, and layer k contains $\binom{L}{k}$ genotypes. For $L = 5$, statements (iii) and (iv) imply that there can be at most two double or triple mutants that are peaks, or one double and one

k	I	II	III
0	1	1	1
1	0	0	0
2	2	2	1
3	0	0	1
4	1	0	0
5	0	1	1
total	4	4	4

TABLE 2. Distinct peak patterns with the maximal number of peaks for fitness landscapes with $L = 5$ that induce the staircase triangulation.

triple mutant. Additionally one peak can be placed in layer 0 or 1 and another one in layer 4 or 5. Table 2 lists all peak patterns with the maximal number of peaks that are allowed based on the statements (i)-(iv), up to symmetries. They all have 4 peaks. \square

Open question: What is the maximal number of peaks of a fitness landscape that induces the staircase triangulation for arbitrary L ?

3.4. Staircase triangulations in random fitness landscapes and empirical data. The occurrence of the staircase triangulation in random fitness landscapes with uniformly distributed fitness was investigated by simulations as described in Section 2.2. For $L = 3$ roughly 1/8 of all landscapes induce a staircase triangulation (type 6), see Figure 6 and [30], but for $L = 4$ this triangulation appears to be exceedingly rare. Among 16,000 random samples we could not find a single instance of this triangulation.

To assess how common staircase triangulations are in nature, we analyzed a protein fitness landscape presented in [32]. This landscape comprises all 160,000 sequences that can be generated by varying four loci of protein G domain B1 (GB1) using all 20 amino acid alleles at each site. GB1 is an immunoglobulin-binding protein expressed in Streptococcal bacteria and has a total of 56 amino acids. The four chosen sites contain 12 of the top 20 positively epistatic interactions among all pairwise interactions. The fitness of each sequence was determined by both its stability (i.e. the fraction of folded proteins) and its function (i.e. binding affinity to Immunoglobulin) and was measured by coupling mRNA display with Illumina sequencing. The distribution of the fitness is extremely skewed, with the majority of sequences having a very small fitness, while very few sequences have a very high fitness.

Since the present analysis is focused on bi-allelic fitness landscapes, we examined bi-allelic sub-landscapes of the protein landscape of [32]. This we did by starting from any arbitrary sequence in the genotype space and then considering all the $2^4 = 16$ sequences that can be generated by mutating each locus to a different amino acid. For each locus, we have 19 other possibilities to mutate to, so the number of such sub-landscapes is enormously large. Therefore, we limited our analysis to 10,000 such sub-landscapes. The triangulation imposed by each sub-landscape was computed using the

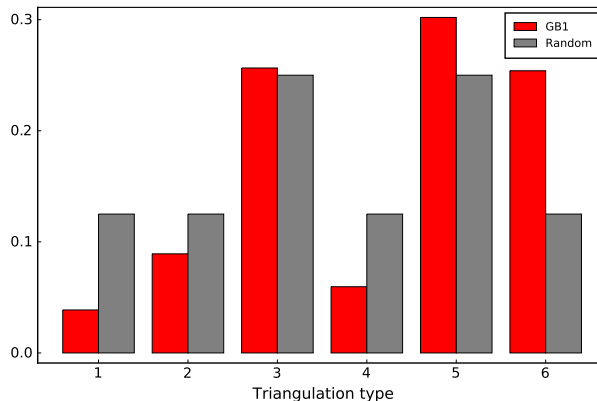


FIGURE 6. Distribution of triangulation types for 3-locus random fitness landscapes with uniformly distributed fitness (grey bars) and biallelic 3-locus sublandscapes of the GB1 protein fitness landscape of [32]. The probabilities for the random landscapes are close to the simple rationals $\frac{1}{8}, \frac{1}{8}, \frac{1}{4}, \frac{1}{8}, \frac{1}{4}, \frac{1}{8}$ [30].

software Macaulay 2. For triangulations that displayed the maximal number of 24 simplices we checked if the vertices of each of the simplices represented paths from the zero string 0000 to its antipodal sequence 1111. Upon doing so, we found at least 45 landscapes that showed staircase triangulations and all of them had either one or two peaks. All 360 3-locus sub-landscapes of these 45 landscapes also show triangulations of type 6, i.e. staircase triangulations.

We additionally determined the empirical distribution over triangulation types of 10,000 3-locus sub-landscapes in the GB1 data and compared this with the corresponding distribution for 10,000 random landscapes (Figure 6). The fraction of landscapes of types 1, 2 and 4 are reduced in comparison to random landscapes, whereas those of types 3, 4 and 6 are enriched. Most notable is the enrichment of landscapes of type 6. Given that the mutated loci in the GB1 data were explicitly chosen because of their positive epistatic interactions, the strong overrepresentation of staircase triangulations in the empirical sub-landscapes with 3 and 4 loci confirms the link to universal positive epistasis and demonstrates the biological relevance of this concept.

4. CIRCUITS, GRÖBNER BASES AND THE STAIRCASE TRIANGULATION

A triangulation can be described explicitly by a list of inequalities, or by its minimal non-faces (Chapter 9.4 [8]). In brief, let J be a subset of the vertices of the L -cube. Then J is a minimally dependent point set if there is an affine dependence relation $\sum_{g \in J} \lambda_g g = 0$, $\lambda_v \in \mathbb{R}$, with $\sum_{g \in J} \lambda_g = 0$ and J is minimal with this property. The expression $\sum_{g \in J} \lambda_g w_g$ is called a *circuit*, or a circuit interaction. A minimal non-face is a set of genotypes that does not belong to any simplex in the triangulation, such that the set is minimal with this property.

One can compare the descriptions for the staircase triangulation (Definition 1). The minimal non-faces for $L = 3$ are

$$\begin{aligned} &\{100, 010\}, \{100, 001\}, \{100, 011\} \\ &\{010, 001\}, \{010, 101\}, \{001, 110\} \\ &\{110, 011\}, \{110, 101\}, \{101, 011\}. \end{aligned}$$

The triangulation can also be defined by the circuit signs:

$$\begin{aligned} w_{000} + w_{110} - w_{100} - w_{010} &> 0 \\ w_{000} + w_{101} - w_{100} - w_{001} &> 0 \\ w_{000} + w_{011} - w_{010} - w_{001} &> 0 \\ w_{001} + w_{111} - w_{101} - w_{011} &> 0 \\ w_{010} + w_{111} - w_{110} - w_{011} &> 0 \\ w_{001} + w_{111} - w_{101} - w_{011} &> 0. \end{aligned}$$

The six circuit signs imply the inequalities:

$$\begin{aligned} w_{111} + w_{000} - w_{110} - w_{001} &> 0 \\ w_{111} + w_{000} - w_{101} - w_{010} &> 0 \\ w_{111} + w_{000} - w_{011} - w_{100} &> 0. \end{aligned}$$

The nine inequalities listed correspond exactly to all minimal non-faces (the two rightmost genotypes that appear on each line are the genotypes in the minimal non-faces).

Lemma 1. *The minimal non-faces for the staircase triangulation consists of the sets*

$$\{g, g'\} \text{ such that } g' \not\subseteq g, g \not\subseteq g'.$$

Proof. Each pair $\{g, g'\}$ as above is a minimal non-face. Let S be the set of such pairs. Let $\{g_1 \dots g_r\}$ be a minimal non-face. The genotypes g_1, \dots, g_r do not all belong to the same simplex, which excludes that the genotypes form a chain $g_1 \subseteq \dots \subseteq g_r$. It follows that $g_i \not\subseteq g_j$ and $g_j \not\subseteq g_i$ some pair i, j , and consequently that $\{g_i, g_j\}$ is a non-face. One concludes that $\{g_1, \dots, g_r\} = \{g_i, g_j\}$, which implies that $\{g_1, \dots, g_r\} \in S$. \square

Observation 9. *If a fitness landscape has universal positive epistasis, then the landscape induces the staircase triangulation.*

Proof. It is sufficient to show that the triangulation induced by the fitness landscape has the same minimal non-faces as the staircase triangulation. Let S be the set of pairs

$$\{g, g'\} \text{ such that } g' \not\subseteq g, g \not\subseteq g'.$$

By assumption, the landscape has universal positive epistasis so that

$$w_{g \cup g'} + w_{g \cap g'} \geq w_g + w_{g'}$$

for any two genotypes g, g' . If $\{g, g'\} \in S$, the inequality is strict. It follows that every element in S is a minimal non-face. Moreover, a non-face of the triangulation cannot consist of genotypes that constitute a chain. By an argument similar to the proof of the previous result, it follows that S is the set of minimal non-faces. Since a landscape with universal positive epistasis has the same minimal non-faces as the staircase triangulation, the result follows. \square

One can use Gröbner bases [14] for finding all minimal non-faces of a triangulation (Chapter 9.4 [8]).

Example 2. Let $k[x_{00}, x_{10}, x_{01}, x_{11}]$ and $k[x_0, x_1, y_0, y_1]$ be polynomial rings, and let φ be the map defined by

$$\varphi: \quad x_{00} \mapsto x_0y_0, \quad x_{10} \mapsto x_1y_0 \quad x_{01} \mapsto x_0y_1, \quad x_{11} \mapsto x_1y_1$$

Let $I = \ker \varphi$. Then I is the ideal generated by $x_{11}x_{00} - x_{10}x_{01}$.

Let

$$w = (w_{00}, w_{10}, w_{01}, w_{11})$$

be a weight vector and let $J = \text{in}_{-w}(I)$ be the initial ideal with respect to $-w$ (notice the sign here, $-w$ defines the monomial order). If

$$w_{11} + w_{00} - w_{10} - w_{01} > 0,$$

then $J = (x_{10}x_{01})$.

According to theory on Gröbner bases and triangulation, the generators of J corresponds exactly to the minimal non-faces of the triangulation. One concludes that $\{10, 01\}$ is the only minimal non-face and therefore that the triangulation induced by w consists of the simplices $\{00, 10, 11\}$ and $\{00, 01, 11\}$.

The following result follows immediately from Sturmfels' correspondence, see Theorem 9.4.5 in [8].

Lemma 2. Let $k[x_g]$ be the polynomial ring in variables labeled by the genotypes x_g and let w be the weight vector that defines the fitness landscape. Let $I \subset k[x_g]$ be the defining ideal (as in the previous example). If $J = \text{in}_{-w}(I)$ is square free, then the generators of J correspond exactly the minimal non-faces of the triangulation.

The following result is useful for computational purposes.

Theorem 2. Let S be the set consisting of all elements of the form

$$x_g \cdot x_{g'} - x_{g \vee g'} \cdot x_{g \wedge g'},$$

where g and g' are genotypes such that $g' \not\subset g$ and $g \not\subset g'$. Consider the monomial order defined by a fitness landscape that induces the staircase triangulation. With notation as in Example 2, the set S is a Gröbner basis for the defining ideal $I \subset k[x_g]$.

Proof. Let I be the defining ideal and let $J = \text{in}_{-w}(I)$. It is easy to verify that S generates I . Let $x_{g_1} \cdots x_{g_k}$ be a generator for J . It is sufficient to show that the generator is divisible by a leading term of S .

By the previous lemma, the set $\{g_1 \dots g_k\}$ is a minimal non-face of the triangulation. By Lemma 1,

$$\{g_1 \dots g_k\} = \{g_i, g_j\}$$

where $g_i \not\subset g_j$ and $g_j \not\subset g_i$. By construction, the element

$$x_{g_i}x_{g_j} - x_{g_i \vee g_j} \cdot x_{g_i \wedge g_j} \in S.$$

It follows that $x_{g_1} \cdots x_{g_k}$ is divisible by $x_{g_i}x_{g_j}$ and consequently that

$$x_{g_1} \cdots x_{g_k} = x_{g_i}x_{g_j}.$$

□

Remark 5. For S in the previous theorem, $|S| = 2^{L-1}(2^L + 1) - 3^L$. By construction, $|S|$ equals the number of minimal non-faces.

Proof. According to Lemma 1, $|S|$ is the number of pairs of genotypes g, g' that are neither subsets nor supersets of each other. A genotype g with k 1's has $2^k - 1$ subsets and $2^{L-k} - 1$ supersets. The number of other genotypes that are neither subsets nor supersets of g is therefore

$$n_k = 2^L - 1 - (2^k - 1 + 2^{L-k} - 1) = 2^L - 2^k - 2^{L-k} + 1.$$

Multiplying this with the number of genotypes of size k , summing over k and dividing by 2 to avoid overcounting of pairs one arrives at

$$|S| = \frac{1}{2} \sum_{k=1}^{L-1} \binom{L}{k} n_k = 2^{L-1}(2^L + 1) - 3^L.$$

□

For $L = 4$ the Gröbner basis described in the theorem can be given explicitly (see below). The theorem was applied for verifying that the fitness landscape in Example 1 induces the staircase triangulation.

Gröbner basis for $L = 4$:

$$\begin{aligned}
 &x_{1011} \cdot x_{0111} - x_{0011} \cdot x_{1111}, & x_{1101} x_{0111} - x_{0101} \cdot x_{1111}, \\
 &x_{1110} \cdot x_{0111} - x_{0110} \cdot x_{1111}, & x_{1101} \cdot x_{1011} - x_{1001} \cdot x_{1111}, \\
 &x_{1110} \cdot x_{1011} - x_{1010} \cdot x_{1111}, & x_{1110} \cdot x_{1101} - x_{1100} \cdot x_{1111}, \\
 &x_{1001} \cdot x_{0111} - x_{0001} \cdot x_{1111}, & x_{1010} \cdot x_{0111} - x_{0010} \cdot x_{1111}, \\
 &x_{1100} \cdot x_{0111} - x_{0100} \cdot x_{1111}, & x_{0101} \cdot x_{1011} - x_{0001} \cdot x_{1111}, \\
 &x_{0110} \cdot x_{1011} - x_{0010} \cdot x_{1111}, & x_{1100} \cdot x_{1011} - x_{1000} \cdot x_{1111}, \\
 &x_{0011} \cdot x_{1101} - x_{0001} \cdot x_{1111}, & x_{0110} \cdot x_{1101} - x_{0100} \cdot x_{1111}, \\
 &x_{1010} \cdot x_{1101} - x_{1000} \cdot x_{1111}, & x_{0011} \cdot x_{1110} - x_{0010} \cdot x_{1111}, \\
 &x_{0101} \cdot x_{1110} - x_{0100} \cdot x_{1111}, & x_{1001} \cdot x_{1110} - x_{1000} \cdot x_{1111}, \\
 &x_{1000} \cdot x_{0111} - x_{0000} \cdot x_{1111}, & x_{0100} \cdot x_{1011} - x_{0000} \cdot x_{1111}, \\
 &x_{0010} \cdot x_{1101} - x_{0000} \cdot x_{1111}, & x_{0001} \cdot x_{1110} - x_{0000} \cdot x_{1111}, \\
 &x_{0101} \cdot x_{0011} - x_{0001} \cdot x_{0111}, & x_{0110} \cdot x_{0011} - x_{0010} \cdot x_{0111}, \\
 &x_{1001} \cdot x_{0011} - x_{0001} \cdot x_{1011}, & x_{1010} \cdot x_{0011} - x_{0010} \cdot x_{1011}, \\
 &x_{1100} \cdot x_{0011} - x_{0000} \cdot x_{1111}, & x_{0110} \cdot x_{0101} - x_{0100} \cdot x_{0111}, \\
 &x_{1001} \cdot x_{0101} - x_{0001} \cdot x_{1101}, & x_{1010} \cdot x_{0101} - x_{0000} \cdot x_{1111}, \\
 &x_{1100} \cdot x_{0101} - x_{0100} \cdot x_{1101}, & x_{1001} \cdot x_{0110} - x_{0000} \cdot x_{1111}, \\
 &x_{1010} \cdot x_{0110} - x_{0010} \cdot x_{1110}, & x_{1100} \cdot x_{0110} - x_{0100} \cdot x_{1110}, \\
 &x_{1010} \cdot x_{1001} - x_{1000} \cdot x_{1011}, & x_{1100} \cdot x_{1001} - x_{1000} \cdot x_{1101}, \\
 &x_{1100} \cdot x_{1010} - x_{1000} \cdot x_{1110}, & x_{0100} \cdot x_{0011} - x_{0000} \cdot x_{0111}, \\
 &x_{1000} \cdot x_{0011} - x_{0000} \cdot x_{1011}, & x_{0010} \cdot x_{0101} - x_{0000} \cdot x_{0111}, \\
 &x_{1000} \cdot x_{0101} - x_{0000} \cdot x_{1101}, & x_{0001} \cdot x_{0110} - x_{0000} \cdot x_{0111}, \\
 &x_{1000} \cdot x_{0110} - x_{0000} \cdot x_{1110}, & x_{0010} \cdot x_{1001} - x_{0000} \cdot x_{1011}, \\
 &x_{0100} \cdot x_{1001} - x_{0000} \cdot x_{1101}, & x_{0001} \cdot x_{1010} - x_{0000} \cdot x_{1011}, \\
 &x_{0100} \cdot x_{1010} - x_{0000} \cdot x_{1110}, & x_{0001} \cdot x_{1100} - x_{0000} \cdot x_{1101}, \\
 &x_{0010} \cdot x_{1100} - x_{0000} \cdot x_{1110}, & x_{0010} \cdot x_{0001} - x_{0000} \cdot x_{0011}, \\
 &x_{0100} \cdot x_{0001} - x_{0000} \cdot x_{0101}, & x_{1000} \cdot x_{0001} - x_{0000} \cdot x_{1001}, \\
 &x_{0100} \cdot x_{0010} - x_{0000} \cdot x_{0110}, & x_{1000} \cdot x_{0010} - x_{0000} \cdot x_{1010}, \\
 &x_{1000} \cdot x_{0100} - x_{0000} \cdot x_{1100}
 \end{aligned}$$

ACKNOWLEDGMENTS

This work was initiated by a mini-symposium at the 2019 SIAM Conference on Applied Algebraic Geometry. We thank Lisa Lamberti for organizing this symposium, for many useful discussions, and for a careful reading of our manuscript. We also thank Muhittin Mungan and Anna Seigal for helpful remarks.

Notation	Mathematical term	Biological term
$\{0, 1\}^L$	Bit strings of length L	The set of 2^L genotypes in a biallelic L-locus system
g_i	i :th position of the bit string g	Locus i of genotype g
$g_i = 1$		g has a 1-allele at locus i
$[0, 1]^L$	Unital L -dimensional hypercube	Genotype for a biallelic L -locus system (terminology used in the shape theory)
$g, g' \in \{0, 1\}^L : g - g' = d$	Vertices with distance d in the undirected cube graph	Genotypes with Hamming distance d
	If d (as above) is 1	The genotypes g and g' are mutational neighbors
$w : \{0, 1\}^L \rightarrow \mathbb{R}_{\geq 0}; g \mapsto w(g) = w_g$		Fitness landscape
	Acyclic directed hypercube graphs induced by fitness landscapes	Fitness graphs: the vertices represent genotypes and edges between mutational neighbors are directed towards genotypes with higher fitness.
	A vertex g is a sink in the fitness graph if all edges incident to g are directed towards g .	A genotype g is a peak in the fitness landscape (and fitness graph) if all mutational neighbors of g have strictly lower fitness than g .
	The triangulation of $[0, 1]^L$ induced by the fitness landscape	The shape of the fitness landscape

TABLE 3. Dictionary of commonly used terms.

REFERENCES

- [1] N. BEERENWINKEL, L. PACTER, AND B. STURMFELS, *Epistasis and shapes of fitness landscapes*, *Statistica Sinica*, (2007), pp. 1317–1342.
- [2] K. CRONA, *Polytopes, graphs and fitness landscapes*, in *Recent Advances in the Theory and Application of Fitness Landscapes*, Springer, 2014, pp. 177–205.
- [3] K. CRONA, *Rank orders and signed interactions in evolutionary biology*, *Elife*, 9 (2020), p. e51004.
- [4] K. CRONA, A. GAVRYUSHKIN, D. GREENE, AND N. BEERENWINKEL, *Inferring genetic interactions from comparative fitness data*, *Elife*, 6 (2017), p. e28629.
- [5] K. CRONA, D. GREENE, AND M. BARLOW, *The peaks and geometry of fitness landscapes*, *Journal of theoretical biology*, 317 (2013), pp. 1–10.
- [6] K. CRONA, M. LUO, AND D. GREENE, *An uncertainty law for microbial evolution*, *Journal of theoretical biology*, 489 (2020), p. 110155.
- [7] S. G. DAS, S. O. DIREITO, B. WACLAW, R. J. ALLEN, AND J. KRUG, *Predictable properties of fitness landscapes induced by adaptational tradeoffs*, *Elife*, 9 (2020), p. e55155.
- [8] J. DE LOERA, J. RAMBAU, AND F. SANTOS, *Triangulations, volume 25 of algorithms and computation in mathematics*, 2010.
- [9] J. A. G. DE VISSER AND J. KRUG, *Empirical fitness landscapes and the predictability of evolution*, *Nature Reviews Genetics*, 15 (2014), pp. 480–490.
- [10] J. A. G. DE VISSER, S.-C. PARK, AND J. KRUG, *Exploring the effect of sex on empirical fitness landscapes*, *the american naturalist*, 174 (2009), pp. S15–S30.
- [11] J. DOMINGO, P. BAEZA-CENTURION, AND B. LEHNER, *The causes and consequences of genetic interactions (epistasis)*, *Annual review of genomics and human genetics*, 20 (2019), pp. 433–460.
- [12] H. EBLE, M. JOSWIG, L. LAMBERTI, AND W. LUDINGTON, *Higher-order interactions in fitness landscapes are sparse*, arXiv preprint arXiv:2009.12277, (2020).
- [13] H. EBLE, M. JOSWIG, L. LAMBERTI, AND W. B. LUDINGTON, *Cluster partitions and fitness landscapes of the drosophila fly microbiome*, *Journal of mathematical biology*, 79 (2019), pp. 861–899.
- [14] R. FRÖBERG, *An introduction to Gröbner bases*, John Wiley & Sons, 1997.
- [15] A. L. GOULD, V. ZHANG, L. LAMBERTI, E. W. JONES, B. OBADIA, N. KORASIDIS, A. GAVRYUSHKIN, J. M. CARLSON, N. BEERENWINKEL, AND W. B. LUDINGTON, *Microbiome interactions shape host fitness*, *Proceedings of the National Academy of Sciences*, 115 (2018), pp. E11951–E11960.
- [16] J. HALDANE AND C. WADDINGTON, *Inbreeding and linkage*, *Genetics*, 16 (1931), p. 357.
- [17] S. HERRMANN, M. JOSWIG, AND D. E. SPEYER, *Dressians, tropical grassmannians, and their rays*, in *Forum Mathematicum*, vol. 26, De Gruyter, 2014, pp. 1853–1881.
- [18] S. KAUFFMAN AND S. LEVIN, *Towards a general theory of adaptive walks on rugged landscapes*, *Journal of theoretical Biology*, 128 (1987), pp. 11–45.
- [19] A. KAZNATCHEEV, *Computational complexity as an ultimate constraint on evolution*, *Genetics*, 212 (2019), pp. 245–265.
- [20] J. KRUG, *Epistasis and evolution. Oxford Bibliographies in Evolutionary Biology*, ed. Douglas Futuyama, New York: Oxford University Press, forthcoming.
- [21] C. LIENKAEMPER, L. LAMBERTI, J. DRAIN, N. BEERENWINKEL, AND A. GAVRYUSHKIN, *The geometry of partial fitness orders and an efficient method for detecting genetic interactions*, *Journal of mathematical biology*, 77 (2018), pp. 951–970.
- [22] C. A. MACKEN, P. S. HAGAN, AND A. S. PERELSON, *Evolutionary walks on rugged landscapes*, *SIAM Journal on Applied Mathematics*, 51 (1991), pp. 799–827.
- [23] P. S. MARA, *Triangulations for the cube*, *Journal of Combinatorial Theory, Series A*, 20 (1976), pp. 170–177.
- [24] J. PELLERIN, K. VERHETSEL, AND J.-F. REMACLE, *There are 174 subdivisions of the hexahedron into tetrahedra*, *ACM Transactions on Graphics (TOG)*, 37 (2018), pp. 1–9.

- [25] F. J. POELWIJK, D. J. KIVIET, D. M. WEINREICH, AND S. J. TANS, *Empirical fitness landscapes reveal accessible evolutionary paths*, Nature, 445 (2007), pp. 383–386.
- [26] F. J. POELWIJK, V. KRISHNA, AND R. RANGANATHAN, *The context-dependence of mutations: a linkage of formalisms*, PLoS computational biology, 12 (2016), p. e1004771.
- [27] F. J. POELWIJK, S. TĂNASE-NICOLA, D. J. KIVIET, AND S. J. TANS, *Reciprocal sign epistasis is a necessary condition for multi-peaked fitness landscapes*, Journal of theoretical biology, 272 (2011), pp. 141–144.
- [28] B. SCHMIEGELT AND J. KRUG, *Evolutionary accessibility of modular fitness landscapes*, Journal of Statistical Physics, 154 (2014), pp. 334–355.
- [29] A. SEIGAL AND G. MONTÚFAR, *Mixtures and products in two graphical models*, arXiv preprint arXiv:1709.05276, (2017).
- [30] M. SRIVASTAVA, *Epistasis, shapes and evolution*, master’s thesis, Universität zu Köln, 2018.
- [31] D. M. WEINREICH, R. A. WATSON, AND L. CHAO, *Perspective: sign epistasis and genetic constraint on evolutionary trajectories*, Evolution, 59 (2005), pp. 1165–1174.
- [32] N. C. WU, L. DAI, C. A. OLSON, J. O. LLOYD-SMITH, AND R. SUN, *Adaptation in protein fitness landscapes is facilitated by indirect paths*, Elife, 5 (2016), p. e16965.

¹ DEPARTMENT OF MATHEMATICS AND STATISTICS, AMERICAN UNIVERSITY, WASHINGTON, DC, UNITED STATES

Email address: `kcrona@american.edu`

² INSTITUTE FOR BIOLOGICAL PHYSICS, UNIVERSITY OF COLOGNE, 50937 KÖLN, GERMANY

Email address: `jkrug@uni-koeln.de`

³ DEPARTMENT OF ENVIRONMENTAL SYSTEMS SCIENCE, ETH ZÜRICH, 8092 ZÜRICH, SWITZERLAND

Email address: `malvika.srivastava@env.ethz.ch`